Appl. Magn. Reson. 31, 375–386 (2007)

**Applied Magnetic Resonance**



# Two-Dimensional ELDOR in the Study of Model and Biological Membranes

**Y.-W. Chiang, A. J. Costa-Filho*, and J. H. Freed**

Baker Laboratory of Chemistry and Chemical Biology, and National Biomedical Center for Advanced ESR Technology, Cornell University, Ithaca, New York, USA

Received July 5, 2006; revised September 28, 2006

**Abstract.** Recent studies on model and biological membranes by two-dimensional (2-D) electron–electron double resonance (ELDOR) are reviewed and discussed. The studies include (1) the phase behavior of dispersions of phospholipid-cholesterol membrane vesicles; (2) the effect of the ion-channel-forming peptide gramicidin A on the lipid membrane; and (3) the effects of stimulation by antigen of the immunoglobulin E receptors in plasma membrane vesicles upon the lipid structure. In the first studies it is shown that the 2-D ELDOR spectra enable clear distinctions amongst the different phases, and this leads to a reliable temperature and composition-dependent phase diagram. In the second studies it is possible to distinguish bulk and boundary lipids and to describe their different dynamic structures. In the third studies we could distinguish both liquid-ordered and liquid-disordered spectral components, and one finds that the fraction of the latter increases as a result of stimulation. Emphasis is placed on the new "full Sc− method" of processing the 2-D ELDOR data to significantly enhance spectral resolution, which is particularly important in studying the spectra from coexisting phases or components. In the full Sc− method, one utilizes both the real and imaginary parts of the signal, instead of their magnitude; the needed phase corrections are obtained as part of the nonlinear least-squares fitting of the 2-D ELDOR data.

In 1956 George Feher introduced the first double resonance experiment into electron spin resonance (ESR), namely, electron–nuclear double resonance (ENDOR) [1]. Later, in 1964 Hyde and Maki showed that ENDOR could be performed in liquids [2], and Freed (1965) offered an explanation for it on the basis of electron spin relaxation pathways [3]. The notion of double resonance in liquid samples containing organic radicals was extended to electron–electron double resonance (ELDOR) by Hyde, Chien, and Freed in 1968 [4]. Both ENDOR and

* Present address: Departamento de Física e Informática, Instituto de Física de São Carlos, Universidade de São Paulo, São Carlos, Brazil

ELDOR have flourished since then and have encompassed modern pulse techniques. In this article we provide an overview of some recent developments using two-dimensional (2-D) ELDOR, which was introduced by Gorcester and Freed in 1986 [5]. It is a pulsed 2-D Fourier transform experiment akin to 2-D exchange nuclear magnetic resonance (NMR) first introduced by Ernst and coworkers in 1979 [6]. This experiment is the equivalent of an ELDOR experiment wherein both observing and pumping ESR frequencies are swept. In 2-D ELDOR, very short pulses are used which simultaneously excite all the frequencies in the ESR spectrum in a coherent fashion. This leads to auto-peaks which provide the normal ESR spectral lines and cross-peaks between all pump and observing frequencies.

The sequence of π/2-pulses and respective time delays are shown in Fig. 1. The 2-D spectrum is obtained by Fourier transforming with respect to the times $t_1$ and $t_2$. The "real-time" evolution of the 2-D ELDOR spectrum is obtained by stepping out the mixing-time $T_m$. The analysis of 2-D ELDOR spectra has in the past relied on performing theoretical fitting to experimental data in the magnitude mode to avoid the need for substantial phase corrections. One of the key features in the present review is to report our recent progress in developing a new spectral fitting method, i.e., performing spectral fitting, wherein real and imaginary parts of the complex signal are considered, rather than the traditional magnitude mode. We call this the "full Sc− method". This new method also supplies the phase corrections which may be used to convert the raw experimental data to the absorption spectrum. Thus the full Sc− method provides significantly greater resolution in the spectral features. These matters are discussed below.

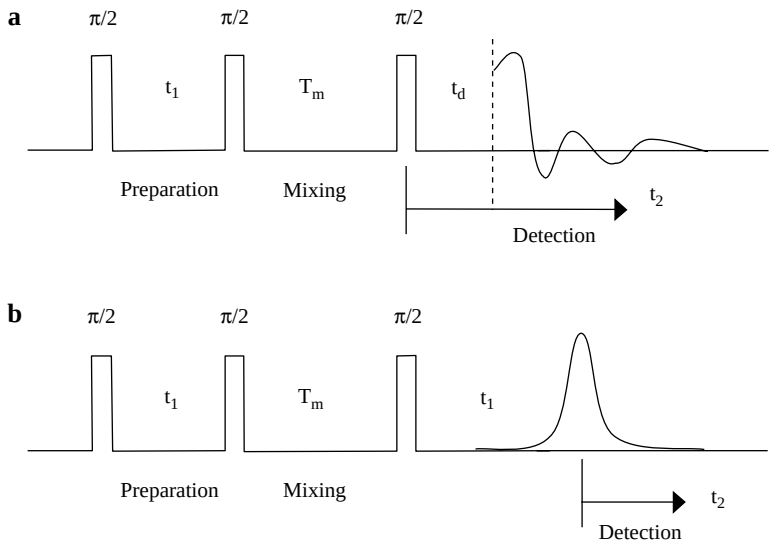


**Fig. 1.** Three π/2-pulse sequence of 2-D ELDOR experiments in the standard 2-D ELDOR (**a**) and SECSY (**b**) formats.



In recent years it has been shown that 2-D ELDOR experiments on spin-labeled lipids in membranes provide much greater spectral resolution to dynamics and ordering in these complex fluids than continuous-wave (CW) ESR spectra are capable of [7, 8]. In a study of several different types of spin-labeled lipids in membrane vesicles, it was shown recently that when they are in the ordinary liquid crystalline or liquid-disordered ($L_d$) phase their 2-D ELDOR spectra are markedly different from those in the liquid-ordered ($L_o$) phase, which is obtained by adding substantial amounts of cholesterol to the phospholipid. This is illustrated in the contour plots shown in Fig. 2. Not only do these 2-D ELDOR spectra enable discrimination of these subtly different phases by simple pattern recognition, they lead to a quantitative assessment of their differences in mem-

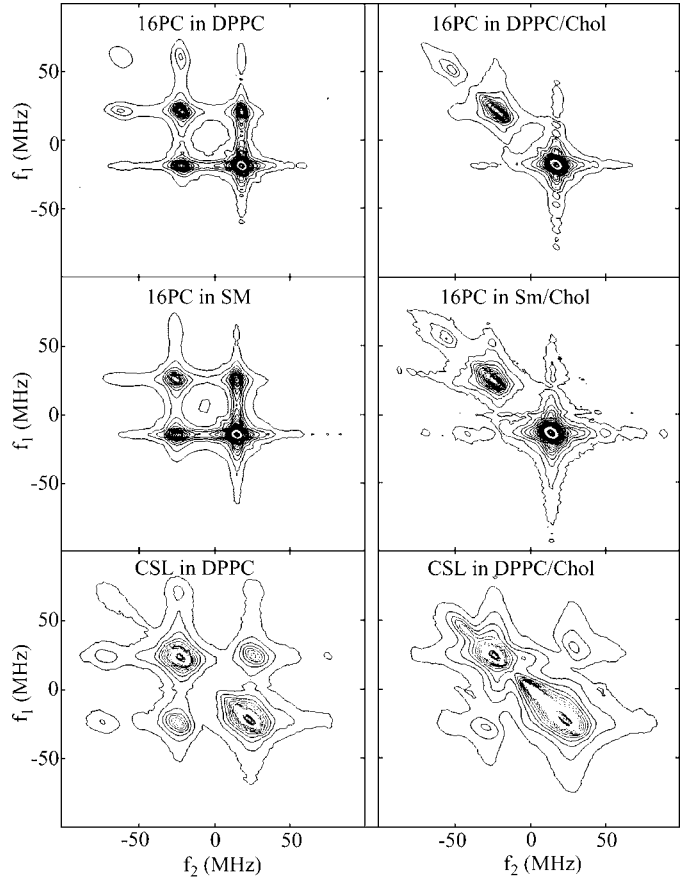


**Fig. 2.** Contour plots of the magnitude 2-D ELDOR spectra at 17.3 GHz ($T_m$ = 500 ns) from spin labels 16-PC, which is an end-chain labeled phospholipid, and cholestane (CSL), which is a cholesterol analogue, at 50 °C for the $L_d$ phase (left) and the $L_o$ phase (right) for several different lipid-cholesterol vesicles. DPPC is dipalmitoyl-phosphatidylcholine and SM is sphingomyelin (from ref. 9).

brane structure and dynamics at a molecular level [9]. In another paper, it was shown that 2-D ELDOR can be very useful in the study of lipid–protein interactions [10]. The 2-D ELDOR spectra of the end-chain spin label 16-PC in lipid vesicles containing the peptide gramicidin A (GA), which forms a dimer ion channel, is composed of two components which are assigned to the bulk lipids (with sharp auto-peaks and cross-peaks) and to the boundary lipids in proximity to the peptide (with broad auto-peaks). This is shown in Fig. 3 for a range of gramicidin A concentrations and temperatures. The quantitative analysis of these spectra shows relatively faster motions and very low ordering in the bulk lipids, whereas the boundary lipids show very high ordering of the sort that implies a significant bend at the end of the acyl chain and slower motion.

In the previous 2-D ELDOR studies, shown in Figs. 2 and 3, the magnitude spectra were used. This is because imperfect spectral coverage from pulses of finite widths and finite spectrometer deadtimes lead to spectral phase shifts with respect to both frequency dimensions, which distort the spectra. The magnitude spectra, however, are not affected by such phase shifts. But, as is well known, magnitude spectra significantly reduce the spectral resolution, so it would be desirable to overcome this issue. Past efforts have included the work of Gorcester and Freed [11], who utilized a linear prediction method that works well for spectra that are

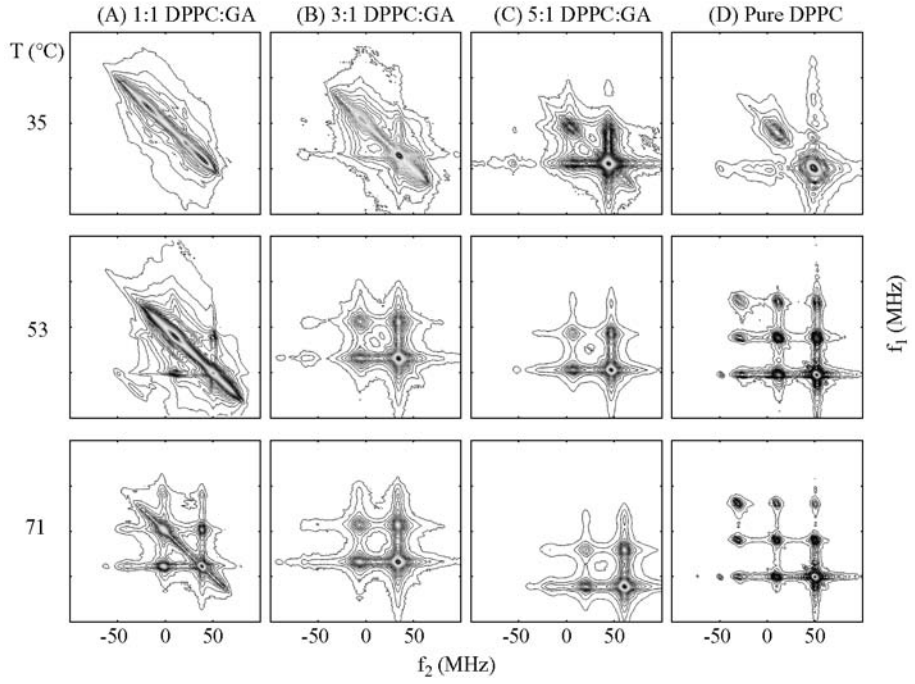


**Fig. 3.** Contour plots of the magnitude 2-D ELDOR spectra at 17.3 GHz ($T_m$ = 1600 ns) from 16-PC for different ratios of DPPC to GA at 35, 53, and 71 °C (from ref. 10).



homogeneously broadened, as well as the method developed by Saxena and Freed [12] for very slow motional spectra which are predominantly inhomogeneously broadened. The intermediate situation of comparable homogeneous and inhomogeneous broadening is not adequately dealt with by either of these two approaches. In fact, the 2-D ELDOR spectra shown in Figs. 2 and 3 fall into this latter category, and this is generally the case for spin-labeled lipids in membranes (especially given the presence of unresolved proton superhyperfine splittings).

The new full Sc− method that we have developed is applicable to 2-D spectra for any arbitrary admixture of homogeneous and inhomogeneous broadening (Y.-W. Chiang et al., unpubl.) [13]. We now explain this method. A standard CW or free induction decay signal is composed of real and imaginary parts, wherein by convention we refer to the absorption as the real part and the dispersion as the imaginary part. A 2-D spectrum thus has real and imaginary parts with respect to both frequencies. That is, it is “hypercomplex”. It can be readily separated into two separate 2-D ELDOR spectra, each of which has a real and an imaginary part. One of them represents the coherence pathway corresponding to that of an echolike signal and is referred to as the Sc− signal. The other represents the coherence pathway with no refocusing, thus corresponding to a free induction signal, and is referred to as the Sc+ signal. The latter, in the presence of significant inhomogeneous broadening, decays more rapidly, often greatly reducing its amplitude after the finite spectrometer deadtime. As a result, the Sc− signal is much more useful in such cases. Nevertheless, the phase problem still makes it difficult to separate out the absorptive and dispersive components, so one normally resorts to the magnitude mode, wherein the phase issue is irrelevant, as noted above.

The full Sc− method utilizes both the real and imaginary components of the experimental Sc− signal, and it includes the phase corrections as additional fitting parameters in the nonlinear least-squares fitting of theory to experiment. For this purpose the standard NLLS package [14] was modified so that the real and imaginary parts of the Sc− spectrum are fitted simultaneously to obtain the dynamic and ordering parameters. This provides much greater sensitivity in the fitting than the much broader magnitude spectra, which had previously been used. Since the fitting also yields the phase corrections, one can then use them to produce pure absorption spectra from the original experimental data, which are helpful for further visual analysis. (These absorption spectra are only approximate, since the phase corrections can only be rigorously applied to the theoretical expressions for the eigenmodes of the stochastic Liouville equation [SLE], which are referred to as the dynamic spin packets [15]. The SLE is the basis for the NLLS fitting [14].)

This full Sc− method is illustrated in Fig. 4. Figure 4a and b shows the real and imaginary parts of the experimental Sc− spectrum before any phase corrections are made. The magnitude spectrum obtained directly from Fig. 4a and b is shown in Fig. 4c. After introducing phase corrections obtained in the fitting, one is able to obtain the absorption spectrum shown in Fig. 4d. Figure 4c and d is shown both as stack plots and contour plots. The much improved resolution of

the 2-D absorption spectra compared with the magnitude spectra is clearly visible. The reader should note that the 2-D ELDOR spectra in Fig. 4 are formatted in a manner different from those in Figs. 2 and 3. The latter result from the standard format of data acquisition corresponding to Fig. 1a, whereas Fig. 4 is in the SECSY format, which corresponds to Fig. 1b. In actual practice it was obtained from experiments with data collected according to Fig. 1a followed by a shear transformation of the data, which is equivalent [16]. In the SECSY mode the auto-peaks are along the $f_1 = 0$ axis (compare Fig. 4) instead of being along the diagonal (compare Figs. 2 and 3). The full Sc−

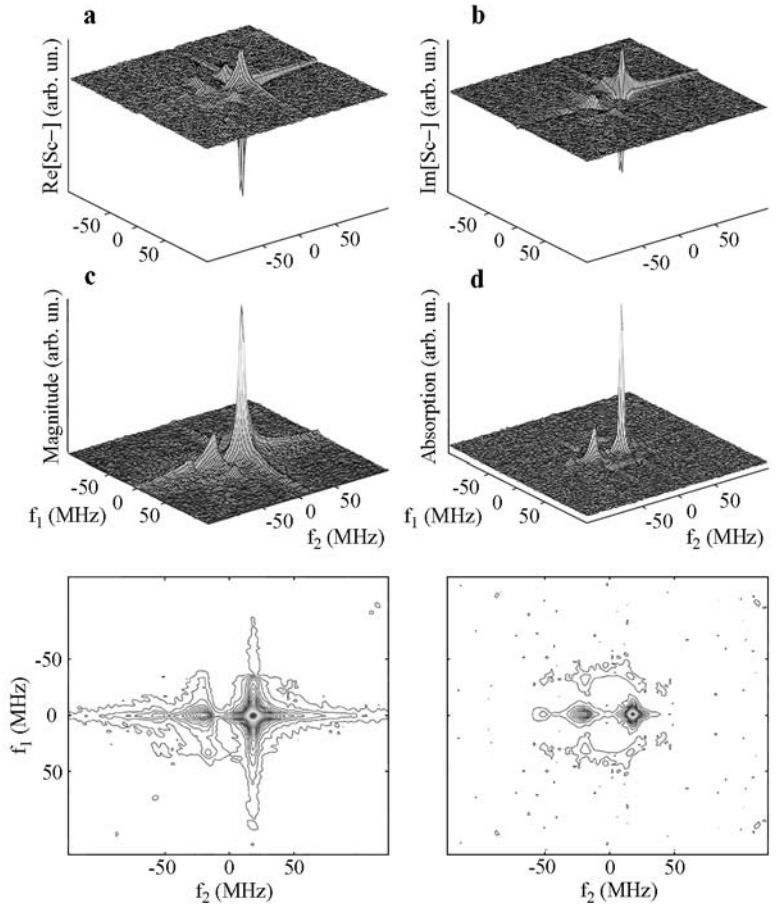


**Fig. 4.** 2-D ELDOR spectra at 17.3 GHz ($T_m$ = 50 ns) of 16-PC in unstimulated plasma membrane vesicles at 30 °C displayed in the full Sc− domain the real (**a**) and the imaginary parts (**b**) of the Sc− signal in the SECSY format. The motivation of obtaining the pure absorption spectrum is clearly demonstrated by comparing the magnitude-mode spectrum (**c**) with the absorption-mode spectrum (**d**), where the latter shows much better spectral resolution. In **c** and **d** both stack-plots and contour plots are shown. The experimental conditions in this and the subsequent figures are as follows: 4 ns π/2 pulses; deadtimes of ca. 35 ns; $t_1$'s ($t_2$'s) stepped out in steps of 2 ns (1 ns).



method may readily be applied to the results shown in Figs. 2 and 3 (and other previous studies). A better discrimination between inhomogeneous and homogeneous broadenings would then be obtained to quantitatively (e.g., $T_2$) describe the respective spectral components. In the following we apply the full Sc− method to recent experimental results which pose greater challenges in interpretation than those in Figs. 2 and 3.

We have chosen two important applications to membrane studies of the full Sc− method (Y.-W. Chiang et al., unpubl.) [13]. The first is in the study of the dynamic structure of different phases of model membranes, such as liquid-ordered ($L_o$) and liquid-disordered ($L_d$) phases, which can coexist in two-phase regions of the phase diagram. In the lower-resolution magnitude spectra it was not possible to reliably separate the respective $L_o$ and $L_d$ spectra from the two-component spectrum, but we find that this can be successfully and reliably done using the full Sc− method. The second application is to plasma membrane vesicles extracted from biological cells. In this case one is interested in immunoglobulin E (IgE) receptor signaling in RBL-2H3 mast cells. Here, only with the improved resolution of the full Sc− method was it possible to distinguish the effects on the lipid membrane when the IgE receptors are stimulated by antigen.

In the first application, we have been able to obtain the phase diagram of 1,2-dipalmitoyl-sn-glycero-phosphatidylcholine (DPPC)–cholesterol binary mixtures versus temperature. This phase diagram has regions corresponding to liquid-disordered, liquid-ordered, and gel phases. The 2-D ELDOR spectra from the 16-PC spin label are very distinctive for these phases, especially in the absorption format. We illustrate this in Fig. 5, which shows contour plots for each of these three phases. These are the "normalized" contour plots which are obtained by taking contour plots, such as those in Fig. 4c and d, except that one first divides by the $f_1 = 0$ spectrum, so that the resultant $f_1 = 0$ contour is just a line of unity value. This mode of representation provides a plot of the homogeneous line width (along $f_1$) versus the ESR spectrum (along $f_2$) [15]. One sees that the $L_d$ phase yields normalized contours representing the narrowest line widths, whereas those from the gel phase represent the broadest. In addition, the normalized contours show distinctive patterns of line width variations across the spectrum. A careful analysis of the 2-D ELDOR spectra versus mixing time $T_m$ and temperature has allowed us to characterize the respective single-phase regions as well as the two-phase regions leading to the phase diagram shown in Fig. 6. This phase diagram is in reasonably good agreement with previous studies [17, 18], which however required several different physical techniques as opposed to our application of just 2-D ELDOR. We also show in Fig. 6 typical 2-D ELDOR spectra in the standard magnitude mode (for convenience in presentation) for a few of the points in the phase diagram corresponding to single-phase regions. In addition, with the aid of the full Sc− method, the dynamic parameters could be reliably extracted and used to determine the dynamic structure over the whole phase diagram (Y.-W. Chiang et al., unpubl.) [13].

In the second example, we have applied the full Sc− method to analyze the 2-D ELDOR spectra we obtained from plasma membrane vesicles (PMV) from

RBL-2H3 mast cells (e.g. Fig. 4) in order to investigate the dynamic phase structural changes upon antigen cross-linking of IgE receptors on the surface of the PMV [19]. The 2-D ELDOR spectra after stimulation show small but significant changes, whereas the CW ESR do not. We found it difficult to obtain unambiguous fits to the spectra in the magnitude mode with either one or two spectral components. With the new full Sc− method, we have been able to obtain good-quality fits and to distinguish the small but significant changes in the PMV before and after stimulation. The molecular dynamic and ordering parameters extracted from spectral fitting also enable us to characterize the heterogeneities in the PMV.

Unstimulated versus stimulated spectra in the magnitude mode of the standard 2-D ELDOR formats (i.e., ELDOR and SECSY) are shown in Fig. 7 along

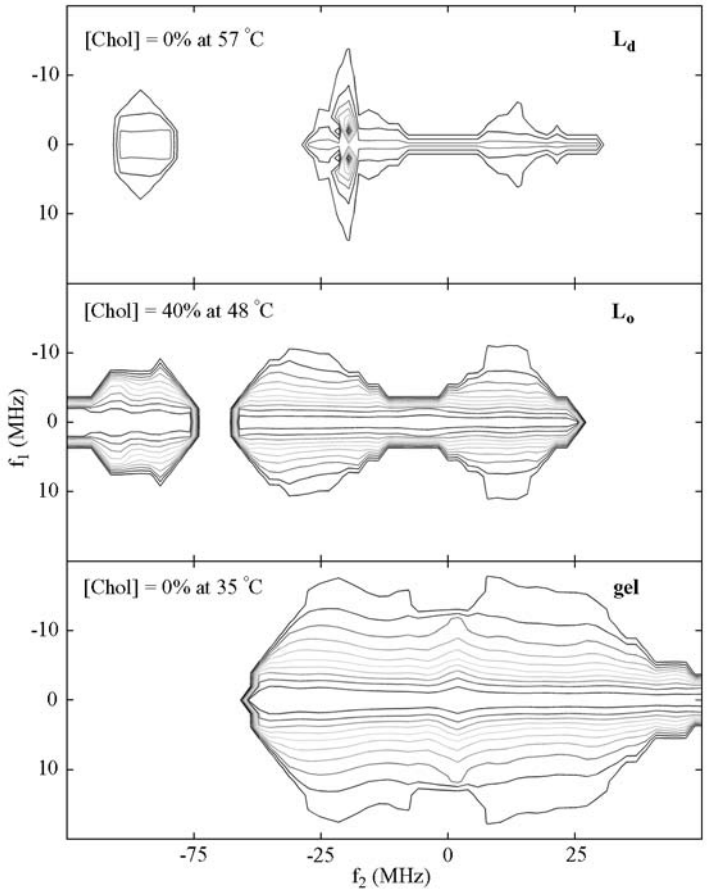


**Fig. 5.** Absorption 2-D ELDOR spectra of 16-PC in DPPC-cholesterol vesicles in the normalized contour presentation, which display the enhanced spectral resolution such that one can observe and study the homogeneous linewidths in the $f_1$ direction. The upper, middle, and lower contours represent $L_d$, $L_o$, and gel phase cases, respectively.



with their difference. We found it necessary to fit the spectra with two spectral components, indicating two coexisting components, in order to achieve good fits to the full Sc− data. The ordering, given by the ordering parameter $S_0$, is found to be the best distinguishing feature between the coexisting components corre-

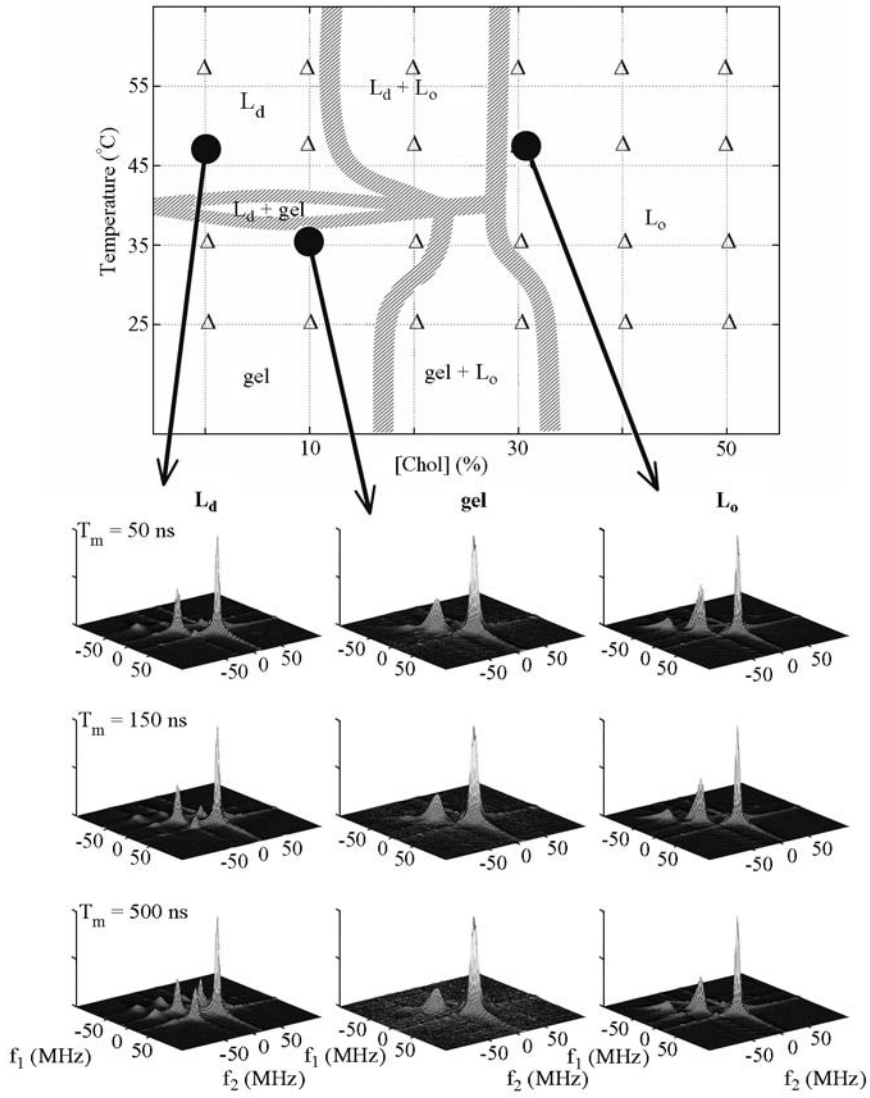


**Fig. 6.** Top, Phase diagram of binary mixtures of DPPC-cholesterol containing 16-PC determined according to 2-D ELDOR analysis. Triangles and filled circles indicate the compositions that were studied. Bottom, 2-D ELDOR spectra, from compositions as marked, show distinctive patterns and line shape variations for one to characterize the membrane phases. (Standard magnitude mode shown for convenience.)

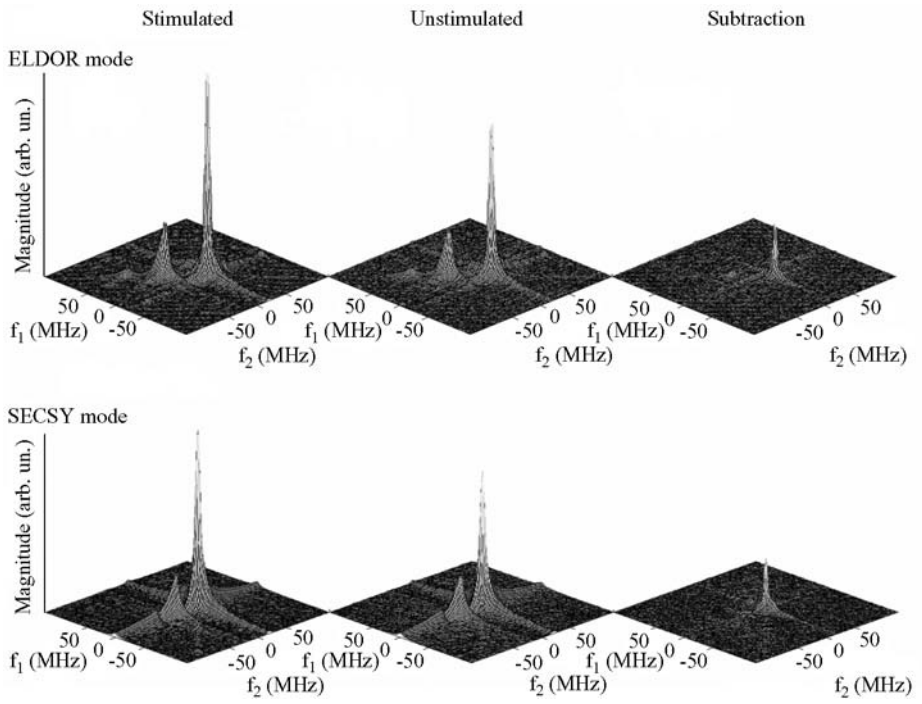


**Fig. 7.** 2-D ELDOR spectra at 17.3 GHz from 16-PC in PMV from RBL-2H3 cells. Unstimulated vs. stimulated spectra (30 °C, $T_m$ = 50 ns) in the magnitude mode of both 2-D ELDOR formats (i.e., ELDOR and SECSY) as well as their difference.

sponding to an $L_d$ and an $L_o$ phase, whereas the rotational diffusion rates ($R_\perp$) for both components are comparable (compare Fig. 8). The coexisting spectral components at $T_m$ = 50 ns and 30 °C in the (SECSY) absorption mode are shown in Fig. 8 in the normalized absorption mode.

The populations of the coexisting components are found to change upon stimulation. As shown in Fig. 9, the population of the $L_o$ phase in both unstimulated and stimulated samples is found to increase modestly with increasing temperature. Upon stimulation, the PMV tends to remodel itself to become more disordered, i.e., the population of the $L_d$ component increases. This result is consistent with the model that Fridriksson et al. [20] proposed for their results from detergent-resistant membranes (DRM) from the same cell line as used for this study. In investigating the phospholipid composition of DRM vesicles isolated from stimulated and unstimulated cells at 37 °C, Fridriksson et al. [20] using mass spectrometry found an increase (12–22%) in the abundance of polyunsaturated phospholipids and a corresponding decrease in the abundance of saturated and monounsaturated species for the DRM from stimulated cells compared to those from unstimulated cells. They proposed that this increase in the abundance of polyunsaturated phospholipids suggests that stimulation causes substantial lipid remod-



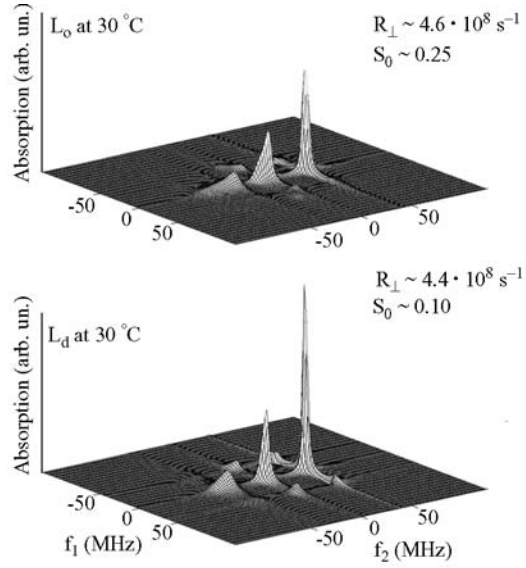


**Fig. 8.** Pure absorption spectral components of 16-PC that represent the coexisting phases in the unstimulated PMV at 30 °C. They represent the best fits to the experimental spectra determined from the full Sc− method. For 16-PC the magnetic parameters are ($A_{xx}$, $A_{yy}$, $A_{zz}$) = (5.0, 5.0, 32.6) in gauss, ($g_{xx}$, $g_{yy}$, $g_{zz}$) = (2.0084, 2.0054, 2.0019).

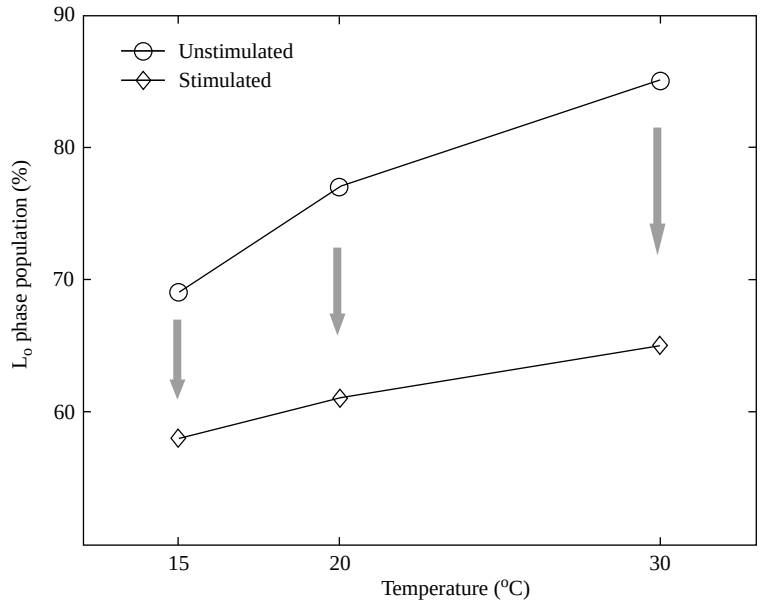


**Fig. 9.** Population of the $L_o$ phase spectral component for unstimulated vs. stimulated PMV as a function of temperature from 2-D ELDOR results using 16-PC spin label.

eling, possibly including the recruitment of intracellular membranes to the plasma membrane. Our results from 2-D ELDOR provide more details about the membrane structural changes before and after cross-linking IgE receptors on the surface of PMV.

## Acknowledgments

We thank Barbara Baird and David Holowka for supplying the PMV samples. This publication was made possible by grant nr. P41RR16292 from the National Center for Research Resources (NCRR) and grant nr. EB03150 from the National Institute of Biomedical and Bioengineering (NIBIB), both are components of the National Institutes of Health (NIH). Its contents are solely the responsibility of the authors and do not necessarily represent the official view of NCRR, NIBIB or NIH.

### Reference

1. Feher G.: Phys. Rev. **103**, 834–835 (1956)
2. Hyde J.S., Maki A.H.: J. Chem. Phys. **40**, 3117–3118 (1964)
3. Freed J.H.: J. Chem. Phys. **43**, 2312–2332 (1965)
4. Hyde J.S., Chen J.C.W., Freed J.H.: J. Chem. Phys. **48**, 4211–4226 (1968)
5. Gorcester J., Freed J.H.: J. Chem. Phys. **85**, 5375–5377 (1986)
6. Jeener J., Meier B.H., Bachmann P., Ernst R.R.: J. Chem. Phys. **71**, 4546–4553 (1979)
7. Lee S., Patyal B.R., Saxena S., Crepeau R.H., Freed J.H.: Chem. Phys. Lett. **221**, 397–406 (1994)
8. Patyal B.R., Crepeau R.H., Freed J.H.: Biophys. J. **73**, 2201–2220 (1997)
9. Costa-Filho A.J., Shimoyama Y., Freed J.H.: Biophys. J. **84**, 2619–2633 (2003)
10. Costa-Filho A.J., Crepeau R.H., Borbat P.P., Ge M., Freed J.H.: Biophys. J. **84**, 3364–3378 (2003)
11. Gorcester J., Freed J.H.: J. Magn. Reson. **78**, 292–301 (1988)
12. Saxena S., Freed J.H.: J. Magn. Reson. **124**, 439–454 (1997)
13. Chiang Y.-W., Ph. D. thesis, Cornell University, Ithaca, USA 2006
14. Budil D.E., Lee S., Saxena S., Freed J.H.: J. Magn. Reson. A **120**, 155–189 (1996)
15. Gorcester J., Millhauser G.L., Freed J.H. in: Modern Pulsed and Continuous Wave Electron Spin Resonance (Kevan L., Bowman M.K., eds.), pp. 119–194. New York: Wiley 1990.
16. Lee S.Y., Budil D.E., Freed J.H.: J. Chem. Phys. **101**, 5529–5558 (1994)
17. Vist M.R., Davis J.H.: Biochemistry **29**, 451–464 (1990)
18. Sankaram M.B., Thompson T.E.: Proc. Natl. Acad. Sci. USA **88**, 8686–8690 (1991)
19. Field K.A., Holowka D., Baird B.: J. Biol. Chem. **272**, 4276–4280 (1997)
20. Fridriksson E.K., Shipkova P.A., Sheets E.D., Holowka D., Baird B., McLafferty F.W.: Biochemistry **38**, 8056–8063 (1999)

**Authors' address:** Jack H. Freed, Baker Laboratory of Chemistry and Chemical Biology, Cornell University, Ithaca, New York 14853, USA
E-mail: jhf@ccmr.cornell.edu